Thiocyanogen Insertion into P−C Bonds of Diphosphinomethanide Complexes, Leading to Rare Functionalized Diphosphine and Tetraphosphine Ligands

Javier Ruiz,*[,†] Roberto Quesada,[†,‡] Marilín Vivanco,[†] Santiago García-Granda,[§] and M. Rosario Díaz[§]

Departamento de Química Orgánica e Inorgánica and Departamento de Química Física y Analítica, Facultad de Química, Universidad de Oviedo, 33071 Oviedo, Spain

Received December 11, 2006

The complex *fac*-[Mn(CN*t*Bu)(CO)$_3${(PPh$_2$)$_2$C−SCN}] (**2**) reacts with thiocyanogen, affording the unstable derivative *fac*-[Mn(CN*t*Bu)(CO)$_3${(PPh$_2$)C(SCN)C(SSCN)N(PPh$_2$)}] (**3**), as a result of the insertion of the pseudohalogen molecule into one of the P−C bonds of the diphosphinomethanide ligand. This complex undergoes intermolecular sulfur−sulfur coupling processes, with elimination of the pseudohalogen molecules (SCN)$_2$, S(CN)$_2$, and (CN)$_2$, to yield a mixture of the dinuclear complexes *fac*-[{Mn(CN*t*Bu)-(CO)$_3$(PPh$_2$)C(SCN)C(NPPh$_2$)}$_2$−S$_n$] (**4**−**6**) linked through polysulfide chains of different lengths. Treatment of these dinuclear disulfide and trisulfide derivatives with 1 or 2 equiv of HBF$_4$ resulted in the sequential protonation of the nitrogen atoms of the ligand, yielding cationic and dicationic complexes, respectively. In the case of monoprotonated disulfide derivatives ^{31}P NMR experiments reveal the existence of an intramolecular proton-transfer process between the endocyclic nitrogen atoms of both metallic fragments. Similar insertion reactions are observed in the treatment of other diphosphinomethanide complexes containing a P$_2$C−S skeleton such as *fac*-[Mn(L)(CO)$_3${(PPh$_2$)$_2$C−SC(S)NMe$_2$}] (**11a**, L = CN*t*Bu; **11b**, L = CO) and *fac*-[Mn(CN*t*Bu)(CO)$_3${(PPh$_2$)$_2$C−S(C$_5$NH$_3$NO$_2$)}] (**12**) with thiocyanogen, yielding new mononuclear derivatives, whose formation implies additionally unusual transposition and cyclization processes. These mononuclear complexes can be protonated on the nitrogen atom by addition of HBF$_4$, affording complexes containing rare functionalized diphosphine ligands.

Introduction

Thiocyanogen, first reported in 1919,[1] is a useful reagent for the preparation of thiocyanate derivatives in both organic synthesis[2] and coordination chemistry,[3] through reaction pathways involving almost exclusively breaking of the sulfur−sulfur bond. Within our studies concerning the reactivity of Mn(I) diphosphinomethanide complexes with halogens and pseudohalogens, we observed that reaction of *fac*-[Mn(CN*t*Bu)(CO)$_3$-{(PPh$_2$)$_2$CH}] (**1**) with thiocyanogen yielded the thiocyanate-substituted diphosphinomethanide complex *fac*-[Mn(CN*t*Bu)(CO)$_3${(PPh$_2$)$_2$C−SCN}] (**2**).[4] This reaction involved the heterolytic cleavage of the S−S bond in the thiocyanogen molecule by the methanide carbon atom, similar to what we found for halogens and other pseudohalogen molecules. In fact, to the best of our knowledge, there is only one reported example of thiocyanogen reactivity which proceeds without the cleavage of the S−S bond, the formation of a 4-H dioxazine by cycloaddition of (SCN)$_2$ and hexafluoroacetone.[5]

We have now found that treatment of **2** and other diphosphinomethanide complexes containing a P$_2$CS skeleton with thiocyanogen proceeds quite differently, leading to the insertion of the pseudohalogen molecule into a P−C bond of the diphosphinomethanide ligand, a reaction which implies the breaking of a rather strong bond without cleavage of the thiocyanogen sulfur−sulfur bond.[6] P−C bond cleavage processes have attracted a great deal of interest, due to their implication in deactivation pathways of phosphine complexes used as homogeneous catalysts.[7] This is a known reaction in

* To whom correspondence should be addressed. E-mail: jruiz@fq.uniovi.es.

† Departamento de Química Orgánica e Inorgánica.

‡ Current address: Departamento de Química Orgánica, Facultad de Ciencias, Universidad Autónoma de Madrid, 28049 Cantoblanco, Spain.

§ Departamento de Química Física y Analítica.

(1) Soderback, E. E. *Justus Liebigs Ann. Chem.* **1919**, *419*, 217.

(2) (a) Guy, R. G. The chemistry of cyanates and their thio derivatives. In *The Chemistry of Functional Groups*; Patai, S., Ed.; Interscience, New York, 1977; Part 2, Chapter 18, p 833. (b) Block, E.; Schwan, A. L. In *Comprehensive Organic Synthesis*; Trost, B. M., Fleming, I., Semmelhack, M. F., Eds.; Pergamon: Oxford, U.K., 1991; Vol. 4, p 348.

(3) See for instance: (a) Bennett, M. A.; Bruce, M. I.; Matheson, T. W. In *Comprehensive Organometallic Chemistry*; Abel, E. W., Stone, F. G. A., Wilkinson, G., Eds.; Pergamon: Oxford, U.K., 1982; Vol. 4, p 705. (b) Bruce, M. I. in ref 3a, Vol. 4, p 883. (d) Odomin, J. D. In ref 3a, Vol. 1, p 289. (d) Puddephatt, R. J. In *Comprehensive Coordination Chemistry*; Wilkinson, G., Gillard, R. D., McCleverty, J. A., Eds.; Pergamon: Oxford, U.K., 1987; Vol. 5, p 887.

(4) Ruiz, J.; Riera, V.; Vivanco, M.; García-Granda, S.; Díaz, M. R. *Organometallics* **1998**, *17*, 4562−4567.

(5) Roesky, H. W.; Homsy, N. K.; Noltemeyer, M.; Sheldrick, G. M. *Angew. Chem.* **1984**, *96*, 1002−1004; *Angew. Chem., Int. Ed. Engl.* **1984**, *23*, 1000−1001.

(6) It is well established that the P−C bonds of diphosphanylmethanide ligands are significantly shorter than P−C single bonds; see for example: (a) Karsch, H. H.; Schier, A. *J. Chem. Soc., Chem. Commun.* **1994**, 2703−2704. (b) Karsch, H. H.; Grauvogl, G.; Kawecki, M.; Bissinger, P.; Kumberger, O.; Schier, A.; Moller, G. *Organometallics* **1994**, *13*, 610−618. (c) Karsch, H. H.; Keller, U.; Gamper, S.; Moller, G. *Angew. Chem.* **1990**, *102*, 297−298; *Angew. Chem., Int. Ed. Engl.* **1990**, *29*, 295−296. (d) Ruiz, J.; Riera, V.; Vivanco, M.; Lanfranchi, M.; Tiripicchio, A. *Organometallics* **1996**, *15*, 1082−1083.

(7) (a) Garrou, P. E. *Chem. Rev.* **1985**, *85*, 171−185. (b) Kong, K. C.; Cheng, C. H. *J. Am. Chem. Soc.* **1991**, *113*, 6313−6315. (c) Morita, D. K.; Stille, J. K.; Norton, J. R. *J. Am. Chem. Soc.* **1995**, *117*, 8576−8581. (d) Goodson, F. E.; Wallow, T. I.; Novak, B. M. *J. Am. Chem. Soc.* **1997**, *119*, 12441−12453.

10.1021/om0611195 CCC: $37.00 © 2007 American Chemical Society
Publication on Web 02/27/2007

Table 1. Selected Spectroscopic Data for Compounds 3−16

compd	IR[a] ν(CN,CO), cm^{-1}	^{31}P{^{1}H} NMR,[b] δ
3	2172 (m), 2147 (w), 2030 (vs), 1967 (s)	70.8 (br), 47.1 (br)
4	2173 (m), 2142 (w), 2025 (vs), 1961 (s)	61.1 (br), 47.2 (br)
5	2174 (m), 2142 (w), 2026 (vs), 1963 (s)	64.6 (br), 47.4 (br)
6	2174 (m), 2142 (w), 2026 (vs), 1963 (s)	67.6 (br), 47.5 (br)
7	2176 (m), 2053 (vs), 2000 (s), 1969 (m)	107.8 (d, $^{2}J_{PP}$ = 61 Hz), 55.2 (d, $^{2}J_{PP}$ = 61 Hz)
8	2176 (m), 2053 (vs), 1998 (s), 1969 (m)	107.8 (br), 55.2 (br)
9	2172 (m), 2143 (w), 2051 (vs), 2033 (vs), 1996 (s), 1973 (s)	87.7 (br), 51.9 (br)
10	2172 (m), 2143 (w), 2052 (vs), 2032 (vs), 1994 (s), 1972 (s)	103.0 (br), 73.4 (br), 52.4 (br), 47.7 (br)
11a	2172 (m), 2015 (vs), 1952 (s), 1934 (s)	24.3 (s)[c]
11b	2074 (s), 1996 (vs), 1963 (s)	20.0 (s)[c]
12	2172 (m), 2015 (vs), 1952 (s), 1934 (s)	23.2 (s)[c]
13a	2172 (m), 2055 (w), 2034 (vs), 1972 (s)	74.2 (d, $^{2}J_{PP}$ = 61 Hz), 30.8 (d, $^{2}J_{PP}$ = 61 Hz)[c]
13b	2084 (s), 2057 (w), 2021 (m), 2000 (vs)	66.0 (br), 25.7 (br)[c]
14	2172 (m), 2142 (w), 2029 (vs), 1966 (s)	69.1 (br), 47.2 (br)[c]
15a	2178 (m), 2052 (vs), 1990 (s)	101.3 (d, $^{2}J_{PP}$ = 62 Hz), 34.0 (d, $^{2}J_{PP}$ = 62 Hz)[c]
15b	2100 (m), 2041(m), 2017 (vs), 1985 (s)	98.5 (br), 30.0 (br)[c]
16	2173 (m), 2052 (vs), 1997 (s)	101.3 (d, $^{2}J_{PP}$ = 88 Hz), 51.6 (d, $^{2}J_{PP}$ = 88 Hz)[c]

[a] In CH_2Cl_2 unless noted otherwise. [b] In CH_2Cl_2/D_2O unless noted otherwise. [c] In $CDCl_3$.

Table 2. Selected Bond Lengths (Å) and Angles (deg) in Compound 4

N(1)−P(1)	1.648(3)	N(2)−C(3)	1.301(5)
N(1)−C(1)	1.298(5)	C(3)−C(4)	1.398(5)
C(1)−C(2)	1.411(5)	P(4)−C(4)	1.785(4)
P(2)−C(2)	1.782(4)	C(3)−S(3)	1.833(4)
C(1)−S(2)	1.824(4)	S(2)−S(3)	2.02(1)
N(2)−P(3)	1.645(3)		
P(1)−Mn(1)−P(2)	85.98(4)	C(1)−S(2)−S(3)	105.3(1)
C(1)−N(1)−P(1)	125.1(3)	C(3)−S(3)−S(2)	103.9(1)
N(1)−C(1)−C(2)	130.8(4)	C(3)−N(2)−P(3)	126.4(3)
N(1)−C(1)−S(2)	116.7(3)	N(2)−C(3)−C(4)	131.8(4)
C(2)−C(1)−S(2)	112.5(3)	N(2)−C(3)−S(3)	114.9(3)
C(1)−C(2)−P(2)	124.7(3)	C(4)−C(3)−S(3)	113.3(2)

Table 3. Selected Bond Lengths (Å) and Angles (deg) in Compound 5

N(1)−P(1)	1.623(8)	N(2)−C(3)	1.30(1)
N(1)−C(1)	1.32(1)	C(3)−C(4)	1.43(1)
C(1)−C(2)	1.43(1)	P(4)−C(4)	1.79(1)
P(2)−C(2)	1.76(1)	C(3)−S(3)	1.829(9)
C(1)−S(2)	1.82(1)	S(2)−S(1)	2.020(4)
N(2)−P(3)	1.629(7)	S(1)−S(3)	2.025(4)
C(1)−N(1)−P(1)	123.4(7)	S(2)−S(1)−S(3)	108.7(2)
N(1)−C(1)−C(2)	129.8(9)	P(3)−Mn(2)−P(4)	83.2(1)
N(1)−C(1)−S(2)	116.8(8)	C(3)−N(2)−P(3)	123.6(7)
C(2)−C(1)−S(2)	113.4(8)	N(2)−C(3)−C(4)	130.4(8)
C(1)−S(2)−S(1)	103.2(4)	N(2)−C(3)−S(3)	117.0(7)
C(1)−C(2)−P(2)	125.1(7)	C(4)−C(3)−S(3)	112.6(7)

metallic clusters bearing phosphine ligands, usually leading to the formation of M−P and M−C bonds.[8] Other coordinated phosphine ligands may display P−C bond activation processes promoted by acid or basic treatments.[9] On the other hand, there are only a handful of reported examples of P−C bond insertions, such as the insertion of nitriles either into the P−C bond of a phosphinidene complex[10] or into a P−C bond of strained three-membered rings of 2*H*-azaphosphirene complexes[11] and the insertion of electron-poor alkynes into a P−C bond of a coordinated phosphine ligand.[12] Herein we report several examples of the unconventional reactivity of thiocyanogen leading to the insertion of this molecule into P−C bonds of coordinated diphosphinomethanide ligands and of the subsequent formation of a number of rare functionalized diphosphine and tetraphosphine ligands. A preliminary communication of this work has been published.[13]

Results and Discussion

Reaction of *fac*-[Mn(CN*t*Bu)(CO)$_3${(PPh$_2$)$_2$C−SCN}] (**2**) with 1 equiv of (SCN)$_2$ yields *fac*-[Mn(CN*t*Bu)(CO)$_3${(PPh$_2$)C(SCN)C(SSCN)N(PPh$_2$)}] (**3**) as a result of the insertion of the pseudohalogen molecule into a P−C bond of the ligand (Scheme 1). Compound **3** was isolated as a white solid and characterized by spectroscopy (Table 1), by elemental analysis, and by FAB mass spectrometry. Compound **3** proved to be unstable when left to stand in solution, slowly decomposing and therefore precluding the preparation of single crystals for X-ray analysis. However, the elution of **3** through an alumina column using CH_2Cl_2/hexane mixtures leads to the formation of the dimetallic complexes **4**−**6**, in an approximate ratio of 6:4:1, respectively. Compounds **4**−**6** are unique polysulfide derivatives that contain a bridging chain of two to four sulfur atoms, and are formally made from the coupling of two molecules of **3** with elimination of the pseudohalogen molecules (SCN)$_2$, S(CN)$_2$, and (CN)$_2$, respectively (Scheme 1).

This result could be compared with the S−S coupling process reported for the related complex [Mn(CO)$_4${(PPh$_2$)$_2$C−S−I}], which allows the formation of the dimetallic disulfide derivative [(CO)$_4$Mn{(PPh$_2$)$_2$C−S−S−C(PPh$_2$)$_2$}Mn(CO)$_4$],[14] with elimination of I$_2$, on passing the complex through an alumina column.[15] Since the formation of **4**−**6** from **3** requires the

(8) See, for example: (a) Xia, C.-G.; Yang, K.; Bott, S. G.; Richmond, M. G. *Organometallics* **1996**, *15*, 4480−4487. (b) Álvarez, M. A.; García, M. E.; Riera, V.; Ruiz, M. A.; Falvello, L. R.; Bois, C. *Organometallics* **1997**, *16*, 354−364. (c) Kabir, S. E.; Miah, Md. A.; Sarker, N. C.; Hussain, G. M. G.; Hardcastle, K. I.; Nordlander, E.; Rosenberg, E. *Organometallics* **2005**, *24*, 3315−3320. (d) Watson, W. H.; Wu, G.; Richmond, M. G. *Organometallics* **2006**, *25*, 930−945.

(9) (a) Geldbach, T. J.; Pregosin, P. S. *Eur. J. Inorg. Chem.* **2002**, *8*, 1907−1918 and references cited therein. (b) Bott, S. G.; Yang, K.; Richmond, M. G.; Talafuse, K. A. *Organometallics* **2003**, *22*, 1383−1390. (c) Quesada, R.; Ruiz, J.; Riera, V.; García-Granda, S.; Díaz, M. R. *Chem. Commun.* **2003**, 1942−1943. (d) Caballero, A.; Jalon, F. A.; Manzano, B. R.; Espino, G.; Perez-Manrique, M.; Mucientes, A.; Poblete, F. J.; Maestro, M. *Organometallics* **2004**, *23*, 5694−5706. (e) Ruiz, J.; García-Granda, S.; Díaz, M. R.; Quesada, R. *Dalton Trans.* **2006**, 4371−4376.

(10) Schiffer, M.; Scheer, M. *Angew. Chem.* **2001**, *113*, 3520−3523; *Angew. Chem., Int. Ed.* **2001**, *40*, 3413−3416.

(11) Streubel, R.; Wilkens, H.; Jones, P. G. *Chem. Eur. J.* **2000**, *6*, 3997−4000.

(12) Yamamoto, Y.; Sugawara, K. *Dalton Trans.* **2000**, 2896−2897.

(13) Ruiz, J.; Quesada, R.; Riera, V.; Vivanco, M.; García-Granda, S.; Díaz, M. R. *Angew. Chem., Int. Ed.* **2003**, *42*, 2392−2395.

(14) Ruiz, J.; Ceroni, M.; Quinzani, O. V.; Riera, V.; Vivanco, M.; García-Granda, S.; Van der Maelen, F.; Lanfranchi, M.; Tiripicchio, A. *Chem. Eur. J.* **2001**, *7*, 4422−4430.

(15) Ruiz, J.; Ceroni, M.; Quinzani, O. V.; Riera, V.; Piro, O. E. *Angew. Chem.* **2001**, *113*, 226−228; *Angew. Chem., Int. Ed.* **2001**, *40*, 220−222.

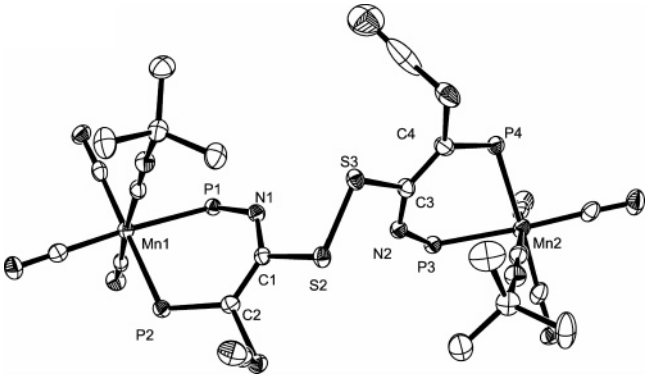

Figure 1. X-ray crystal structure of compound **4** (hydrogen atoms and phenyl groups removed for clarity). Thermal ellipsoids are drawn at the 30% probability level.

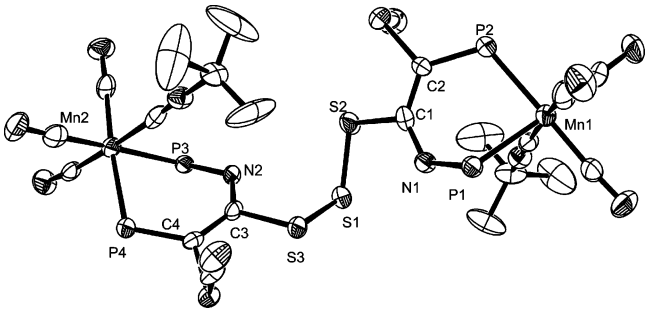

Figure 2. X-ray crystal structure of compound **5** (hydrogen atoms and phenyl groups removed for clarity). Thermal ellipsoids are drawn at the 30% probability level.

scission of two S−S bonds, one S−S bond and one S−C bond, and two S−C bonds, respectively, the relative amount of each compound in the reaction mixture could be explained by considering the weakness of the S−S bond versus the S−C bond in the inserted thiocyanogen molecule. Complexes **4**−**6** are isolated as white solids and have very similar spectroscopic features and solubilities. Thus, the IR spectra for the three species are virtually identical in the CO and CN stretching regions, and the complexes can only be distinguished by the slight differences in the chemical shift of one of the two nonequivalent phosphorus atoms in the $^{31}P\{^{1}H\}$ NMR spectra (see Table 1). Nevertheless, the major species, **4** and **5**, could be separated by chromatographic workup and were fully characterized, including the elucidation of their solid-state structures by X-ray crystallography (Figures 1 and 2 and Tables 2 and 3). The minor product **6** could not be totally purified, as it always contains some amount of **5**; therefore, its characterization is based mainly on the FAB mass spectrum.

The structure of complex **4** (Figure 1) formally contains a thiocyanogen molecule inserted into two P−C(methanide) bonds of two diphosphinomethanide complexes **2**, although, as stated above, its formation implies a stepwise process of S−S bonds breaking and forming. The different bond lengths and angles within the equivalent halves of the molecule are very similar (Table 2). The bond lengths within the skeleton P1−N1−C1−C2−P2 of the expanded chelating ligand are intermediate between single and double bonds, reflecting delocalization of the negative charge of the methanide carbon atom throughout that skeleton. The P3, N2, C3, C4, and P4 atoms are essentially coplanar, with the Mn2 atom out of this plane. The dihedral angle between the planes defined by P3−Mn2−P4 and P3−N2−C3 is 44.28°. The other six-membered metallacycle is twisted, with angles between planes defined by P1−Mn1−P2 and P1−N1−C1 of 47.40°, P1−Mn1−P2 and P2−C2−C1 of 26.50°, and P1−N1−C1 and P2−C2−C1 of 25.41°. The angle between the planes defined by N1−C1−S2 and N2−C3−S3 is 85.46°. The S2−S3 bond length (2.02(1) Å) is slightly shorter than that found in the *cyclo*-octasulfur molecule (2.06 Å), whereas the C−S bond lengths (1.828(4) Å on average) are typical for a single bond. The structure of the trisulfide derivative **5** (Figure 2) is closely related to that of **4**, with one more sulfur atom in the polysulfide chain that links the two diphosphine rings. Bond distances and angles within the two diphosphine rings are very similar to those found for **4**. The S2−S1−S3 angle (108.7(2)°) is in the range usually found for polysulfide compounds. Both metallacycles adopt a disposition similar to that described for compound **4**.

Scheme 1. Synthesis of Compounds 3−6[a]

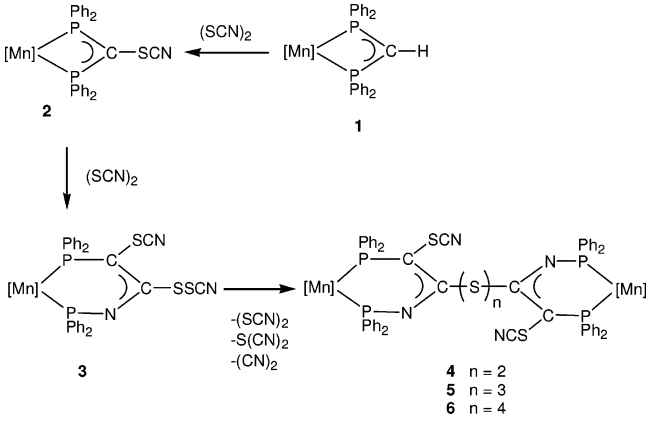

[a] [Mn] = [Mn(CN*t*Bu)(CO)$_3$]$^+$.

Scheme 2. Synthesis of Compounds 7−10[a]

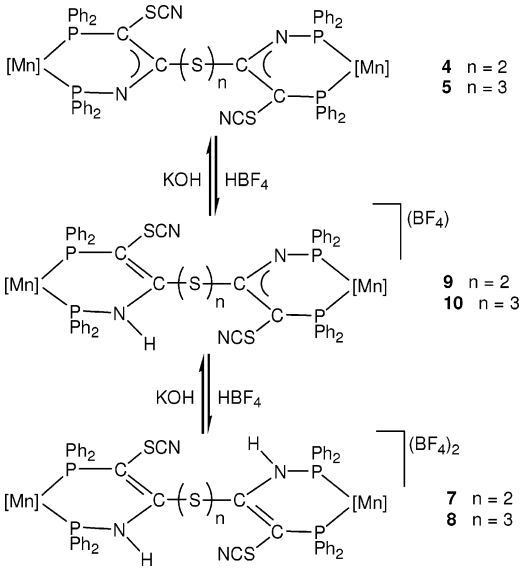

[a] [Mn] = [Mn(CN*t*Bu)(CO)$_3$]$^+$.

Compounds **4** and **5** bear the dianionic bridging ligands $[\{PPh_2C(SCN)CNPPh_2\}_2S_n]^{2-}$ (n = 2, 3), which can be protonated by treatment with HBF_4, yielding the dicationic complexes **7** and **8** (Scheme 2). This process is readily reversible by treating dichloromethane solutions of these derivatives with an excess of solid KOH. Spectroscopic data suggested that the protonation takes place on the nitrogen atom of the diphosphine ligand and not on the original methanide carbon. Thus, IR spectra of these compounds displayed bands characteristic of cationic *fac*-tricarbonyl derivatives, with frequencies notably higher that those exhibited by the related neutral fragments. Moreover, IR spectra recorded in a Nujol dispersion showed a characteristic

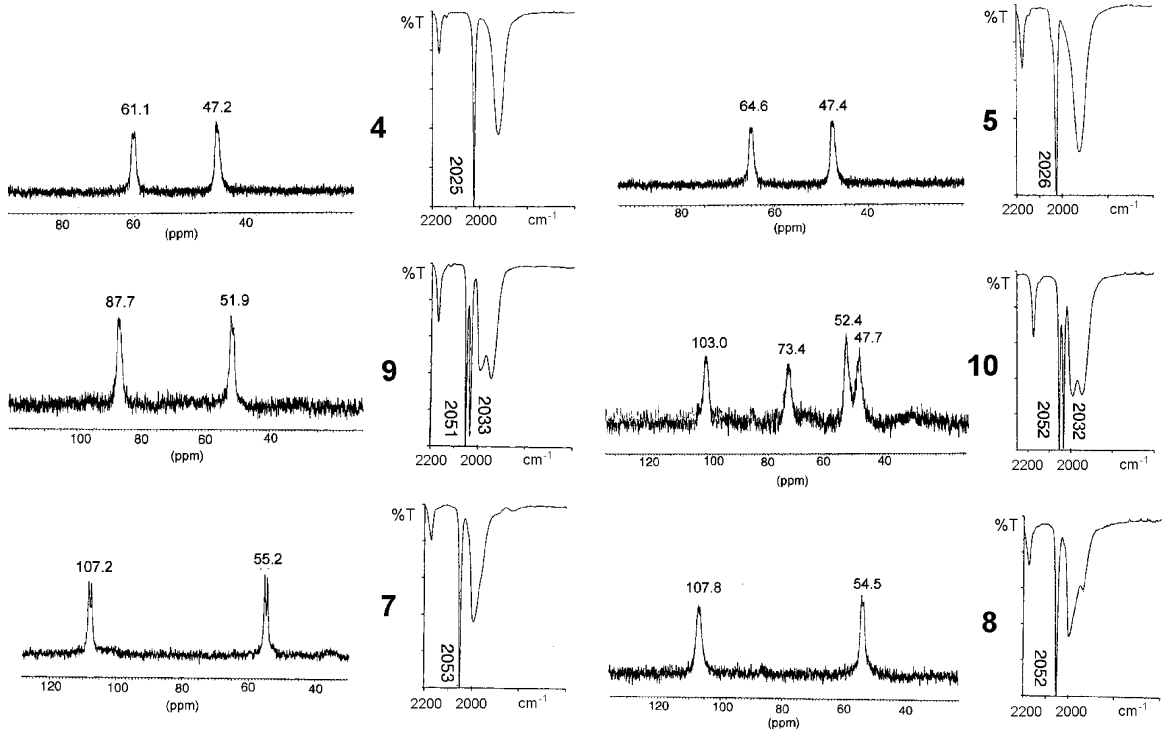

Figure 3. IR (CH_2Cl_2) and $^{31}P\{^1H\}$ NMR (CH_2Cl_2/D_2O) spectra of neutral, cationic, and dicationic disulfide derivatives **4**, **7**, and **9** (left) and neutral, cationic and dicationic trisulfide derivatives **5**, **8**, and **10** (right).

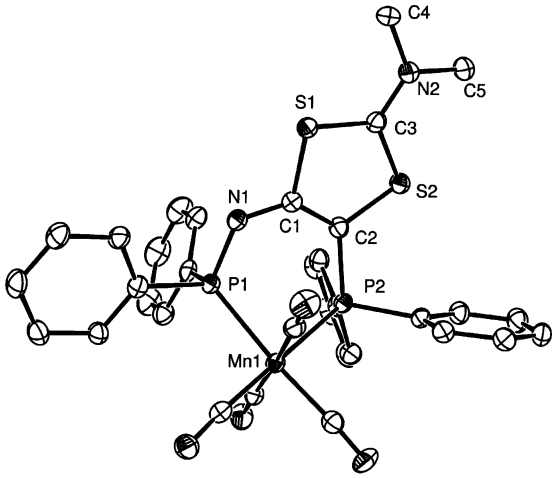

Figure 4. X-ray crystal structure of the complex cation **13b** (hydrogen atoms removed for clarity). Thermal ellipsoids are drawn at the 30% probability level.

band at 3200 cm^{-1} assignable to a N−H group. ^{31}P NMR showed that protonation affected the inequivalent phosphorus atoms of the diphosphine ring very differently. While the chemical shift of the phosphorus bound to the nitrogen atom is shifted downfield to approximately 108 ppm as a result of the protonation of this atom, the other P atom is only slightly affected. In a independent experiment we have found that a mixture of compounds **7** and **8** can be obtained by treatment of the mononuclear derivative **3** with HBF_4. Apparently protonation of the diphosphinomethanide ligand in **3** promotes the elimination of the pseudohalogen molecules $(SNC)_2$ and $S(CN)_2$ with formation of sulfur−sulfur bonds, similarly to what occurs when this compound is eluted through an alumina column. This process resembles that described for $[Mn(CO)_4\{(PPh_2)_2C-S-I\}]$, which is quantitatively converted to the disulfide $[(CO)_4Mn\{(PPh_2)_2C-S-S-C(PPh_2)_2\}Mn(CO)_4]$ by treatment with acid, eliminating I_2.[15]

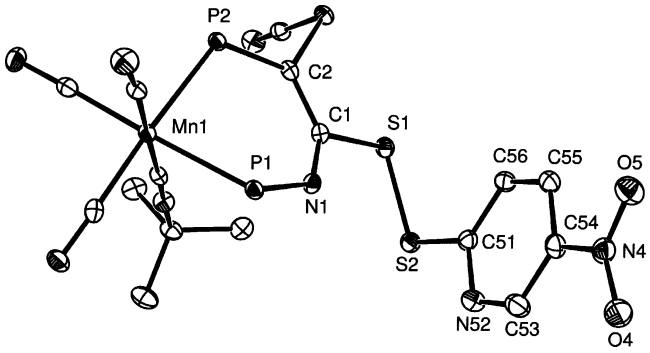

Figure 5. X-ray crystal structure of compound **14** (hydrogen atoms and phenyl groups removed for clarity). Thermal ellipsoids are drawn at the 30% probability level.

More interestingly, neutral complexes **4** and **5** can be selectively protonated on only one of the nitrogen atoms by treatment with 1 equiv of HBF_4 yielding the cationic derivatives **9** and **10** (Scheme 2). Obviously, these complexes can both be protonated again by addition of an additional 1 equiv of HBF_4 to give **7** and **8** or deprotonated by treatment with KOH to regenerate **4** and **5**. The IR spectra of **9** and **10** recorded in a Nujol dispersion showed a band at 3175 cm^{-1} assignable to an N−H group. In solution, the IR spectra showed two sets of bands in the carbonyl stretching region, corresponding to the two *fac*-tricarbonyl fragments present in the molecule. Remarkably, the frequencies of these fragments are slightly different from those corresponding to both the parent neutral **4** and **5** and dicationic **7** and **8** derivatives (Figure 3). Thus, bands assignable to the *fac*-$[Mn(CNtBu)(CO)_3]$ moiety bonded to the anionic fragment of the ligand appear at frequencies (8 and 6 cm^{-1} for **9** and **10**, respectively) higher than those displayed by the neutral **4** and **5**. The bands corresponding to the cationic fragment are much more similar to those observed in **7** and **8**. This effect seems to indicate the existence of a relevant electronic communication through the polysulfide bridge. The

Scheme 3. Synthesis of Compound 12[a]

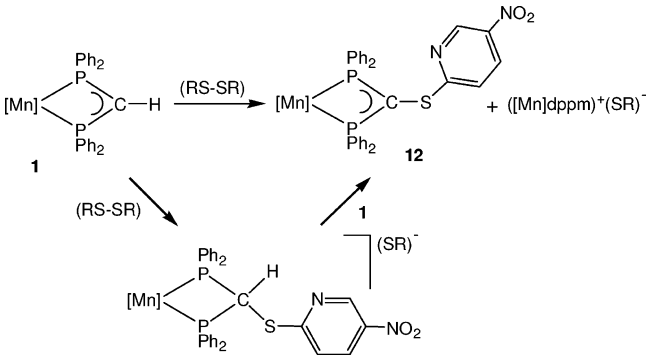

[a] [Mn] = [Mn(CN*t*Bu)(CO)$_3$]$^+$; R = 5-nitropyridine.

Scheme 4. Formation of the Cationic Complexes 13a,b[a]

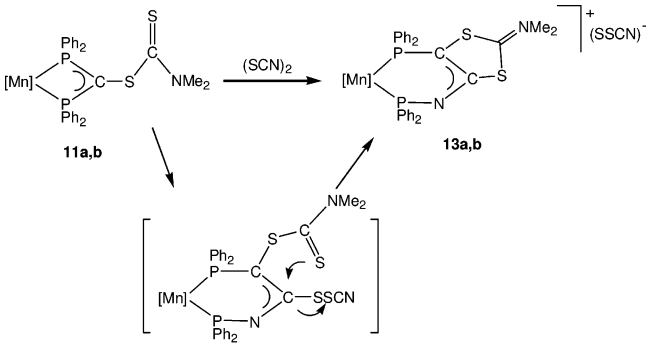

[a] **13a**, [Mn] = [Mn(CN*t*Bu)(CO)$_3$]$^+$; **13b**, [Mn] = [Mn(CO)$_4$]$^+$.

Scheme 5. Synthesis of Compound 14[a]

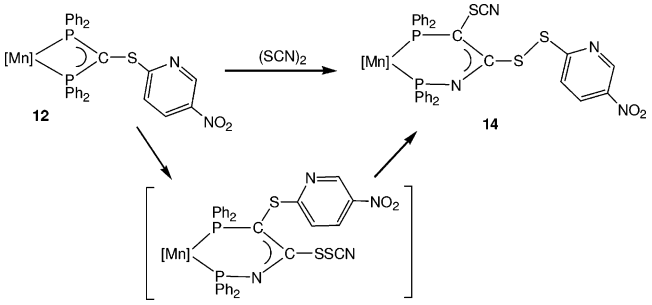

[a] [Mn] = [Mn(CN*t*Bu)(CO)$_3$]$^+$.

disappearance of the π component of the P−C bonds in the metallacycle upon protonation might explain the difference in the reflection of this electronic communication in the IR of both carbonyl fragments. The electronic connection between the two diphosphine rings through the sulfur chain produces a decrease of the basicity in the anionic diphosphine ring once the other is protonated. In fact, this process allows the quantitative generation of compounds **9** and **10** instead of a statistical mixture of neutral (**4** and **5**), monocationic (**9** and **10**), and dicationic (**7** and **8**) complexes when only 1 equiv of acid is added. Moreover, **9** and **10** can alternatively be prepared by mixing equimolecular quantities of neutral **4** and **5** and dicationic **7** and **8**, in dichloromethane as solvent. Although **9** and **10** display very similar IR spectra, ^{31}P NMR experiments reveal significant differences between these derivatives (Figure 3). Trisulfane **10** displayed four signals corresponding to four inequivalent phosphorus atoms at 103.0 and 52.4 ppm, assignable to the protonated part of the ligand, and at 73.4 and 47.7 ppm, corresponding to the other diphosphine ring, in agreement with the situation discussed for the IR spectra. On the other hand, disulfane **9** showed only two signals at 87.5 and 51.9 ppm,

Table 4. Selected Bond Lengths (Å) and Angles (deg) in Compound 13b

N(1)−P(1)	1.631(4)	S(2)−C(3)	1.712(4)
N(1)−C(1)	1.325(5)	S(2)−C(2)	1.750(4)
C(1)−C(2)	1.384(6)	N(2)−C(3)	1.318(6)
P(2)−C(2)	1.784(4)	N(2)−C(4)	1.466(6)
C(1)−S(1)	1.786(4)	N(2)−C(5)	1.454(6)
S(1)−C(3)	1.714(5)		
P(1)−Mn(1)−P(2)	85.76(4)	C(5)−N(2)−C(4)	116. 8(4)
C(3)−S(1)−C(1)	96.2(2)	S(2)−C(3)−S(1)	116.3(2)
C(3)−S(2)−C(2)	96.1(2)	N(1)−C(1)−S(1)	112.3(3)
C(1)−N(1)−P(1)	123.8(3)	C(1)−C(2)−S(2)	117.0(3)
C(3)−N(2)−C(5)	121.6(4)	C(2)−C(1)−S(1)	113.9(3)
C(3)−N(2)−C(4)	121.5(4)	S(2)−C(2)−P(2)	118.3(2)

Table 5. Selected Bond Lengths (Å) and Angles (deg) in Compound 14

N(1)−P(1)	1.653(2)	C(1)−S(1)	1.859(3)
N(1)−C(1)	1.294(4)	S(1)−S(2)	2.034(1)
C(1)−C(2)	1.396(4)	S(2)−C(51)	1.777(3)
P(2)−C(2)	1.792(3)		
P(1)−Mn(1)−P(2)	85.84(4)	N(1)−C(1)−S(1)	114.6(2)
C(1)−S(1)−S(2)	101.3(1)	C(2)−C(1)−S(1)	112.5(2)
C(1)−N(1)−P(1)	127.7(2)	C(1)−C(2)−P(2)	123.2(2)
N(1)−C(1)−C(2)	132.8(3)	C(51)−S(2)−S(1)	103.8(1)

corresponding to average values of the expected chemical shift for the two types of inequivalent phosphorus atoms present in the anionic and neutral fragments of the ligand. This result seems to indicate the existence of an intramolecular proton-transfer process between both rings of the bridging ligand which is rapid on the NMR time scale (Figure 3). This process cannot be completely stopped when the NMR sample is cooled to −80 °C in CD_2Cl_2. At this temperature, ^{31}P{^{1}H} NMR spectra showed a severe broadening of the signals but a new set of four signals could not be seen. The above results show that the mobility of the proton atom is dependent on the length of the sulfur chain, and this can be envisaged in the solid-state structures of **4** and **5**, where the nitrogen atoms are significantly closer in the disulfane **4** (3.600 Å) than in the trisulfane **5** (5.416 Å). This circumstance could allow the proton-transfer process in complex **9** to proceed through an intermediate species featuring an intramolecular N−H···N hydrogen bond, similar to that present in protonated diamines with close nitrogen atoms.[16]

We set out to test the reproducibility of the thiocyanogen insertion into other diphosphinomethanide derivatives bearing similar functionalities. We have previously reported the synthesis of *fac*-[Mn(CN*t*Bu)(CO)$_3${(PPh$_2$)$_2$C−SC(S)NMe$_2$}] (**11a**) by reaction of *fac*-[Mn(CN*t*Bu)(CO)$_3${(PPh$_2$)$_2$C−H}] (**1**) with tetramethylthiuram disulfide.[17] Similarly, **1** readily reacts with other activated disulfides such as 2,2′-dithiobis(5-nitropyridine), yielding a mixture of the functionalized diphosphinomethanide complex **12** and the cationic dppm parent complex, which can be easily separated after chromatographic workup. A likely mechanism for the reaction involves the nucleophilic degradation of the disulfide by the diphosphinomethanide complex followed by deprotonation of the resultant cationic intermediate by the starting material (Scheme 3). Compound **12** was fully characterized spectroscopically (see Experimental Section).

Reaction of *fac*-[Mn(CN*t*Bu)(CO)$_3${(PPh$_2$)$_2$C−SC(S)NMe$_2$}] (**11a**) with 1 equiv of $(SCN)_2$ at room temperature yields the cationic derivative **13a**, which contains a unique unsymmetrical

(16) Mascal, M.; Lera, M.; Blake, A. J.; Czaja, M.; Kozak, A.; Makowski, M.; Chmurzynski, L. *Angew. Chem., Int. Ed.* **2001**, *40*, 3696−3698.

(17) Ruiz, J.; Quesada, R.; Riera, V.; García-Granda, S.; Díaz, M. R. *Chem. Commun.* **2003**, 2028−2029.

Table 6. Crystallographic Data for 4, 5, 13b, and 14

	4	5	13b	14
empirical formula	$C_{70}H_{58}Mn_2N_6O_6P_4S_4$	$C_{70}H_{58}Mn_2N_6O_6P_4S_5$	$C_{34}H_{26}MnN_3O_5P_2S_2$	$C_{42}H_{36}Cl_4MnN_5O_5P_2S_3$
formula wt	1441.27	1473.28	737.58	1045.62
temp (K)	293(2)	293(2)	293(2)	293(2)
wavelength (Å)	1.5418	1.5418	1.5418	1.5418
cryst syst, space group	triclinic, $P\bar{1}$	triclinic, $P\bar{1}$	triclinic, $P\bar{1}$	triclinic, $P\bar{1}$
unit cell dimens				
a (Å)	11.1915(7)	11.2755(4)	10.5186(7)	11.1806(4)
b (Å)	17.3864(7)	16.4423(6)	10.7753(6)	12.5221(6)
c (Å)	18.9243(9)	21.966 (1)	15.022 (1)	17.1308(7)
α (deg)	104.540(3)	72.807(2)	93.073(5)	102.117(3)
β (deg)	94.546(5)	77.227(2)	95.253(4)	94.625(3)
γ (deg)	90.072(5)	72.190(3)	92.24 (4)	102.178(2)
V (Å^3)	3552.3(3)	3665.6(3)	1691.31(18)	2272.52(16)
Z, calcd density (Mg/m^3)	2, 1.347	2, 1.335	2, 1.448	2, 1.528
abs coeff (mm^{-1})	5.281	5.389	5.607	6.901
F(000)	1484	1516	756	1068
cryst size (mm)	0.063 × 0.038 × 0.038	0.200 × 0.050 × 0.025	0.230 × 0.200 × 0.150	0.380 × 0.350 × 0.150
θ range for data collecn (deg)	2.42−69.83	2.91−68.13	2.96−69.9	2.66−69.61
limiting indices	$-13 \le h \le 13$, $-21 \le k \le 20$, $0 \le l \le 23$	$-12 \le h \le 13$, $-18 \le k \le 19$, $0 \le l \le 24$	$-12 \le h \le 12$, $-13 \le k \le 12$, $0 \le l \le 18$	$-13 \le h \le 13$, $-14 \le k \le 14$, $0 \le l \le 20$
no. of rflns collected/unique	26 009/13 309 (R_{int} = 0.068)	21 409/10 418 (R_{int} = 0.126)	16 304/6329 (R_{int} = 0.062)	20 403/8423 (R_{int} = 0.081)
completeness in θ range (%)	99.1	77.7	99	98.5
abs cor	semiempirical from equivalents			
max, min transmissn	0.818, 0.632	0.874, 0.681	0.413, 0.320	0.355, 0.132
refinement method	full-matrix least squares on F^2			
no. of data/restraints/params	13 309/0/947	10 418/0/838	6329/3/438	8423/0/703
goodness of fit on F^2	0.926	0.844	1.106	1.011
final R indices ($I > 2\sigma(I)$)	R1 = 0.051, wR2 = 0.131	R1 = 0.066, wR2 = 0.161	R1 = 0.066, wR2 = 0.200	R1 = 0.051, wR2 = 0.129
R indices (all data)	R1 = 0.073, wR2 = 0.142	R1 = 0.173, wR2 = 0.216	R1 = 0.073, wR2 = 0.207	R1 = 0.056, wR2 = 0.139
largest diff peak, hole (e Å^{-3})	1.248, −0.875	1.272, −0.332	1.656, −0.581	0.806, −0.587

diphosphine ligand featuring a 1,3-dithiol-2-ylidene iminium group. A possible mechanism for the reaction is proposed in Scheme 4. As encountered in the case of **2**, the first step could be the insertion of the pseudohalogen molecule into one of the P−C bonds of the diphosphine, resulting in the expansion of the metallacycle from four to six members. Then, an intramolecular nucleophilic attack of the thiocarbonyl group from the dithiocarbamate fragment to the iminic carbon atom of the diphosphine ring could occur, displacing the $SSCN^-$ anion and resulting in the formation of a dithia heterocycle containing a dimethyliminium group.

Spectroscopic data in solution are in agreement with this structure (see Table 1 and Experimental Section). Thus, the ^{31}P NMR spectrum of **13a** displayed two signals at 72.4 and 30.8 ppm, corresponding to two inequivalent phosphorus atoms. The IR spectrum of this cationic complex showed only a moderate increase in the frequency of the CO stretching bands with respect to the neutral starting complex **11a**, as a result of the zwitterionic nature of the ligand, resulting from the positive charge being situated mainly on the nitrogen atom of the dimethyliminium group and the negative charge delocalized on the metallacycle. All attempts to grow X-ray-quality crystals of **13a** were unsuccessful; therefore, the reaction was repeated employing the parent tetracarbonyl complex $[Mn(CO)_4\{(PPh_2)_2C-SC(S)-NMe_2\}]$ (**11b**). Reaction of **11b** with thiocyanogen proceeded similarly to our previous result, yielding the complex **13b**. Spectroscopic features of this derivative are very similar to those corresponding to **13a**, indicating that the same type of reaction had occurred. The structure of **13b** was determined by X-ray analysis (Figure 4). Bond lengths and angles within the metallacycle are similar to those observed in **4** and **5** (Table 4). A five-membered ring is fused to the metallacycle. This dithiaheterocycle is essentially planar, in which all carbon−sulfur bond distances are slightly smaller than those corresponding to a single bond. Bond angles around the N2 atom are close to 120°, with the C3, C4, and C5 atoms contained in the same plane, supporting a sp^2 hybridization for this atom. Cyanate anion was found as the counterion in the crystal structure. As we discussed in the proposed mechanism, $SSCN^-$ should be displaced and cyanate might be produced in a hydrolysis reaction of this unstable anion.

Some important features of compounds **13a**,**b** should be emphasized. Both species contain an unsymmetrical functionalized diphosphine ligand which is zwitterionic, the functional group holding a 1,3-dithiol-2-ylidene iminium residue. This is rather unusual and could be the starting point for preparing even more sophisticated diphosphines, taking into account that related organic iminium salts have been used for the synthesis of tetrathiafulvalene-based organic conductors and superconductors.[18]

Compound **12** also reacts instantly with 1 equiv of thiocyanogen, yielding a mixture from which the neutral derivative **14** was obtained after chromatographic workup (Scheme 5). The ^{31}P NMR spectrum suggested a similar insertion process of the thiocyanogen molecule into the P−C bond of the ligand, as it showed two signals at 60.1 and 47.2 ppm. The IR spectrum is very similar to that of compound **4**, and a weak band corresponding to a SCN group can be seen at 2142 cm^{-1}. The ^{1}H NMR spectrum of **14** displayed signals characteristic of the 5-nitropyridine group. Confirmation of the structural formulation was unambiguously established by X-ray structural diffraction (Figure 5 and Table 5). Compound **14** crystallized jointly with two molecules of dichloromethane. Structural parameters are

(18) (a) Dahlstedt, E.; Hellberg, J.; Petoral, R. M., Jr.; Uvdal, K. *J. Mater. Chem.* **2004**, *14*, 81−85. (b) Cristau, H. J.; Darviche, F.; Babonneau, M. T.; Fabre, J. M.; Torreilles, E. *Tetrahedron* **1999**, *55*, 13029−13036. (c) Veciana, J.; Rovira, C.; Cowan, D. *Tetrahedron Lett.* **1988**, *29*, 3467−3470. (d) Moore, D. J.; Bryce, M. R. *Synthesis* **1997**, 407−409.

Scheme 6. Protonation Reactions of Compounds 13a,b and 14 To Afford 15a,b and 16, Respectively[a]

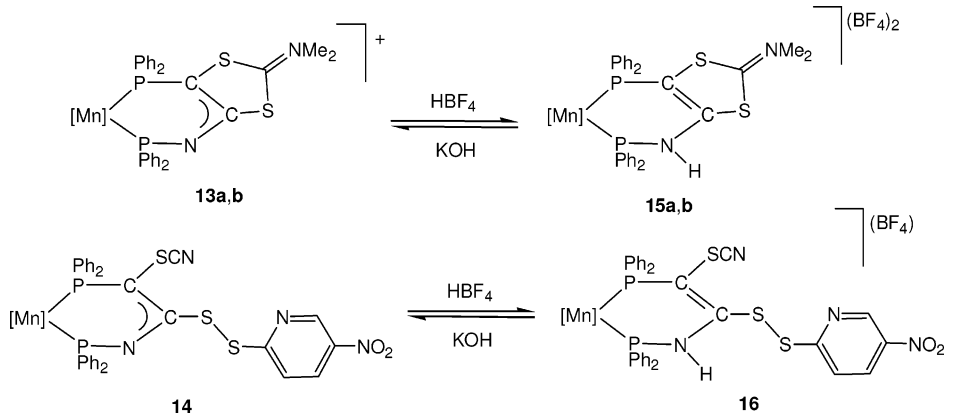

[a] **13a** and **15a**, [Mn] = $[Mn(CNtBu)(CO)_3]^+$; **13b** and **15b**, [Mn] = $[Mn(CO)_4]^+$.

very similar to those found in the case of disulfide **4**, in which one mononuclear fragment is replaced by the organic nitropyridine fragment. It is worth noting that the S1−C1 bond distance (1.850(3) Å) is significantly longer than the S2−C51 bond distance (1.777(3) Å), highlighting the weakness of the first C−S bond. The S1−S2 bond distance (2.0339(11) Å) corresponds to a single bond and is similar to the sulfur−sulfur bond lengths found in **4** and **5**.

Compound **14** could be considered an evolution product from the intermediate species proposed in Scheme 5. Thus, the first step of the reaction should be the insertion of the $(SCN)_2$ molecule into the P−C bond of the original ligand. This would lead to an unstable intermediate, similar to the other examples we have shown. In this case, steric impedance would disfavor the formation of polysulfide chains, leading to the observed result, in which SCN and $S(NC_5H_3NO_2)$ have switched their positions.

Treatment of compounds **13a**,**b** and **14** with HBF_4 yielded the corresponding cationic derivative **15a**,**b** and **16**, respectively (Scheme 6). All spectroscopic data are closely related to those displayed by the doubly protonated polysulfides **7** and **8**. The IR spectra in Nujol dispersion showed a band asignable to a N−H group at 3201 and 3182 cm^{-1}, respectively, reflecting that the protonation takes place on the nitrogen atom of the diphosphine ring, and the CO stretching bands in solution correspond to a cationic derivative. The ^{31}P NMR spectra displayed similar changes upon protonation. The chemical shift of the phosphorus atom bonded to the carbon atom is only lightly affected, whereas the other signal, corresponding to the phosphorus atom bonded to the nitrogen atom, is shifted downfield by approximately 30 ppm (Table 1).

To date, we have only observed insertion of thiocyanogen into the P−C bond of coordinated diphosphinomethanides with ligands containing the P_2CS skeleton. Nevertheless, it is expected that other C-functionalized diphosphinomethanide complexes could exhibit behavior toward thiocyanogen similar to that described in this paper, thus enhancing the synthetic possibilities of these systems.

Conclusion

Reaction of thiocyanogen with coordinated diphosphinomethanide ligands bearing different S−R functionalities resulted in the insertion of the pseudohalogen molecule into a P−C bond of the ligand. This process represents an unprecedented example of insertion into a rather strong P−C bond which occurs instantly at room temperature, without breaking of the S−S bond of the thiocyanogen molecule. The complexes obtained are very reactive and either undergo intermolecular S−S coupling processes, yielding dinuclear complexes linked through polysulfide chains of different lengths, or intramolecular transposition and cyclization processes, giving rare functionalized diphosphinomethanide complexes.

The nitrogen atom inserted into the diphosphine ring can be protonated reversibly by strong acids. In the case of the dinuclear complexes **4** and **5** this protonation is sequential to give the corresponding cationic (**9**, **10**) and dicationic (**7**, **8**) derivatives, highlighting the existence of an electronic communication through the polysulfide chain, as well as of a proton-transfer process dependent on the sulfur chain length. The new diphosphine ligands could pave the way toward even more sophisticated systems, as the presence of a 1,3-dithiol-2-ylidene iminium group in **13a**,**b** suggests.

Experimental Section

General Considerations. All reactions were carried out under nitrogen atmosphere using standard Schlenk techniques. Solvents were dried and purified by standard techniques and distilled under nitrogen prior to use. All reactions were monitored by IR spectroscopy (Perkin-Elmer FT 1720-X and Paragon 1000 spectrophotometers). Elemental analyses were performed on a Perkin-Elmer 240B elemental analyzer. ^1H, ^{13}C, and ^{31}P NMR spectra were recorded using Bruker AC-300 and AC-200 instruments. Chemical shifts are given in ppm relative to internal $SiMe_4$ (^1H) or external 85% H_3PO_4 (^{31}P) references. FAB-MS spectra were provided by the University of Santiago de Compostela Mass Spectrometry Service. *fac*-$[Mn(CNtBu)(CO)_3\{(PPh_2)_2CH\}]$ (**1**),[19] *fac*-$[Mn(CNtBu)(CO)_3\{(PPh_2)_2CSCN\}]$ (**2**),[4] *fac*-$[Mn(CNtBu)(CO)_3\{(PPh_2)_2CSC(S)NMe_2\}]$ (**11a**),[17] and $[Mn(CO)_4\{(PPh_2)_2CSC(S)NMe_2\}]$ (**11b**)[17] were prepared as reported.

Compound 3. A solution containing $(SCN)_2$ (0.027 g, 0.230 mmol) was added dropwise to a solution of **2** (0.15 g, 0.226 mmol) with continuous stirring over 5 min at room temperature. The solution was then concentrated to 2 mL under vacuum. The addition of hexane (10 mL) produced the precipitation of a white solid; yield 85% (0.15 g). Data for **3** are as follows. IR (CH_2Cl_2): ν 2172 m (CN*t*Bu), 2147 w (SCN), 2030 vs, 1967 s cm^{-1} (CO). ^1H NMR (CD_2Cl_2): δ 7.96−7.04 (20H, Ph), 1.50 ppm (s, 9H, *t*Bu). $^{31}P\{^1H\}$ NMR (CH_2Cl_2/D_2O): δ 70.8 (br), 47.1 (br) ppm. FAB-MS (positive ion): *m*/*z* 779 [M^+], 753 [M^+ − CN], 721 [M^+ − SCN], 689 [M^+ − SSCN]. Anal. Calcd for $C_{36}H_{29}MnN_4O_3P_2S_3$: C, 55.53; H, 3.75; N, 7.19. Found: C, 54.58; H, 3.97; N, 6.92.

(19) Ruiz, J.; Riera, V.; Vivanco, M.; García-Granda, S.; García-Fernández, A. *Organometallics* **1992**, *11*, 4077−4082.

Compounds 4−6. Compound **3** (0.10 g, 0.128 mmol) was passed through an alumina column (activity degree III). Elution with CH_2Cl_2/hexane (1:1) afforded **5** along with small amounts of **6**; further elution with CH_2Cl_2/hexane (3:2) afforded **4**. Both fractions were recrystallized in CH_2Cl_2/hexane to give **4** and **5** as colorless crystals. A second recrystallization of the first fraction provided **6** as the major product in the mother liquor. Data for **4** are as follows. Yield: 30% (0.028 g). IR (CH_2Cl_2): ν 2173 m (CN*t*Bu), 2142 w (SCN), 2025 vs, 1961 s cm^{-1} (CO). ^{1}H NMR (CD_2Cl_2): δ 8.70−5.70 (40 H, Ph), 1.60 (s, 18 H, *t*Bu). ^{31}P{^{1}H} NMR (CH_2Cl_2/D_2O): δ 61.1 (s, br), 47.2 (s, br). FAB-MS (positive ion): *m*/*z* 1441 [M$^+$]. Anal. Calcd for $C_{70}H_{58}Mn_2N_6O_6P_4S_4$: C, 58.33; H, 4.06; N, 5.83. Found: C, 58.61; H, 4.17; N, 6.01. Data for **5** are as follows. Yield: 20% (0.019 g). IR (CH_2Cl_2): ν 2174 m (CN*t*Bu), 2142 w (SCN), 2026 vs, 1963 s cm^{-1} (CO). ^{1}H NMR (CD_2Cl_2): δ 8.19−6.97 (40 H, Ph), 1.57 (s, 18 H, *t*Bu). ^{31}P{^{1}H} NMR (CH_2Cl_2/D_2O): δ 64.6 (s, br), 47.4 (s, br). FAB-MS (positive ion): *m*/*z* 1473 [M$^+$]. Anal. Calcd for $C_{70}H_{58}Mn_2N_6O_6P_4S_5$: C, 57.06; H, 3.97; N, 5.70. Found: C, 56.85; H, 4.05; N 5.98. Data for **6** are as follows. IR (CH_2Cl_2): ν 2174 m (CN*t*Bu), 2142 w (SCN), 2026 vs, 1963 s cm^{-1} (CO). ^{31}P{^{1}H} NMR (CH_2Cl_2/D_2O): δ 67.6 (s, br), 47.5 (s, br). FAB-MS (positive ion): *m*/*z* 1505 [M$^+$].

Compound 7. A 50 mg portion (0.035 mmol) of compound **4** was dissolved in 10 mL of dichloromethane, and to this solution 12 μL (0.087 mmol) of HBF_4 (54% diethyl ether complex) was added with stirring. The volume was then reduced to 2 mL, and addition of 10 mL of diethyl ether produced the precipitation of a yellow solid, which was washed with diethyl ether (2 × 5 mL) and dried. Data for **7** are as follows. Yield: 90% (51 mg). IR (CH_2Cl_2): ν 2176 m (CN*t*Bu), 2053 vs, 2000 s, 1969 m cm^{-1} (CO). ^{1}H NMR (CD_2Cl_2): δ 7.90−7.26 (42 H, Ph + 2 × N*H*), 1.28 (s, 18 H, *t*Bu). ^{31}P{^{1}H} NMR (CH_2Cl_2/D_2O): δ 107.8 (d, $^2J_{PP}$ = 67 Hz), 55.2 (d, $^2J_{PP}$ = 67 Hz). Anal. Calcd for $C_{70}H_{60}B_2F_8Mn_2N_6O_6P_4S_4$: C, 52.00; H, 3.74; N, 5.20. Found: C, 51.62; H, 3.93; N, 5.39.

Compound 8. This compound was prepared as detailed above; 9 μL (0.065 mmol) of HBF_4 (54% diethyl ether complex) was added to 40 mg (0.027 mmol) of **5** dissolved in 10 mL of dichloromethane. Data for **8** are as follows. Yield: 90% (51 mg). Anal. Calcd for $C_{70}H_{60}B_2F_8Mn_2N_6O_6P_4S_5$: C, 50.99; H, 3.67; N, 5.10. Found: C, 51.17; H, 3.78; N, 5.30. IR (CH_2Cl_2): ν 2175 m (CN*t*Bu), 2053 vs, 1998 s, 1969 m cm^{-1} (CO). IR (Nujol dispersion): 3204 (ν_{N-H}) cm^{-1}. ^{1}H NMR (CD_2Cl_2): δ 7.80−7.01 (42 H, Ph + 2 × N*H*), 1.34 (s, 18 H, *t*Bu). ^{31}P{^{1}H} NMR (CH_2Cl_2/D_2O): δ 107.8 (s, br), 55.2 (s, br).

Compound 9. A 3 μL portion (0.022 mmol) of HBF_4 (54% diethyl ether complex) was added to 30 mg (0.021 mmol) of **4** dissolved in 10 mL of dichloromethane. Evaporation of solvents yielded a colorless oi, which could be precipitated as a white solid from a CH_2Cl_2/hexane mixture. Data for **9** are as follows. Yield: 90% (29 mg). IR (CH_2Cl_2): ν 2172 m (CN*t*Bu), 2143 w, 2051 vs, 2033 vs, 1996 s, 1973 s cm^{-1} (CO). IR (Nujol dispersion): 3174 (ν_{N-H}) cm^{-1}. ^{1}H NMR (CD_2Cl_2): δ 7.96−6.64 (41 H, Ph + N*H*), 1.55 (s, 18 H, *t*Bu). ^{31}P{^{1}H} NMR (CH_2Cl_2/D_2O): δ 87.7 (s, br), 51.9 (s, br). Anal. Calcd for $C_{70}H_{59}BF_4Mn_2N_6O_6P_4S_4$: C, 54.98; H, 3.89; N, 5.50. Found: C, 54.71; H, 4.05; N, 5.65.

Compound 10. This compound was prepared as above, starting with 30 mg (0.02 mmol) of compound **5** and 3 μL (0.022 mmol) of HBF_4 (54% diethyl ether complex). Data for **10** are as follows. Yield: 90% (29 mg). IR (CH_2Cl_2): ν 2173 m (CN*t*Bu), 2143 w, 2052 vs, 2032 vs, 1994 s, 1972 s cm^{-1} (CO). IR (Nujol dispersion): 3175 (ν_{N-H}) cm^{-1}. ^{1}H NMR (CD_2Cl_2): δ 7.96−6.64 (41H, Ph + N*H*), 1.55 (s, 18H, *t*Bu). ^{31}P{^{1}H} NMR (CH_2Cl_2/D_2O): δ 103.0 (s, br), 73.4 (s, br), 52.4 (s, br), 47.7 (s, br). Anal. Calcd for $C_{70}H_{59}BF_4Mn_2N_6O_6P_4S_5$: C, 53.85; H, 3.81; N, 5.38. Found: C, 53.53; H, 4.17; N, 5.40.

Compound 12. A 100 mg portion (0.165 mmol) of **1** was dissolved in 15 mL of dichloromethane, and 31 mg (0.10 mmol) of 2,2′-dithiobis(5-nitropyridine) was added. The mixture turned orange immediately. After 10 min of stirring the solvent was removed and the oily solid that was obtained was chromatographed through an Alox III column. An orange band was eluted using a 1:1 dichloromethane/hexane mixture, which was collected and the solvent evaporated, giving the desired product as an orange solid. Data for **12** are as follows. Yield: 40% (50 mg). IR (CH_2Cl_2): ν 2172 m (CN*t*Bu), 2015 vs, 1952 s, 1934 s cm^{-1} (CO). ^{1}H NMR ($CDCl_3$): δ 9.02 (d, $^4J_{HH}$ = 3 Hz, H_c), 7.74−7.15 (21 H, Ph + H_b), 6.89 (d, $^3J_{HH}$ = 9 Hz, H_a), 0.77 (s, 9 H, *t*Bu). ^{31}P{^{1}H} NMR ($CDCl_3$): δ 23.2 (s). Anal. Calcd for $C_{34}H_{23}MnN_2O_6P_2S$: C, 60.08; H, 4.25; N, 5.53. Found: C, 60.22; H, 4.36; N, 5.68.

Compound 13a. A solution containing $(SCN)_2$ (0.014 g, 0.138 mmol) was added dropwise to a solution of **11** (0.10 g, 0.138 mmol) in 10 mL of CH_2Cl_2 with continuous stirring over 5 min at room temperature. The solvent was removed under vacuum and the obtained solid purified by column chromatography. Small amounts of starting material were eluted using 50 mL of dichloromethane, and then a brown band was eluted using a MeOH/CH_2Cl_2 (1:10) mixture. The brown solid obtained after evaporation of solvents could be recrystallized by diffusion of ether into a dichloromethane solution of the complex. Data for **13a** are as follows. Yield: 55% (60 mg). IR (CH_2Cl_2): ν 2172 m (CN*t*Bu), 2055 w, 2034 vs, 1972 s cm^{-1} (CO). ^{1}H NMR ($CDCl_3$): δ 7.87−7.28 (20 H, Ph), 1.47 (s, 9 H, *t*Bu). ^{31}P{^{1}H} NMR ($CDCl_3$): δ 74.2 (d, $^2J_{PP}$ = 61 Hz, PPh_2), 30.8 (d, $^2J_{PP}$ = 61 Hz, PPh_2). Anal. Calcd for $C_{38}H_{35}MnN_4O_4P_2S_2$: C, 57.57; H, 4.45; N, 7.07. Found: C, 57.34; H, 4.31; N, 7.10.

Compound 13b. This compound was prepared as above, using 0.10 g (0.149 mmol) of $[Mn(CO)_4\{(PPh_2)_2C-SC(S)NMe_2\}]$ (**11b**) and 0.015 g (0.15 mmol) of thiocyanogen. Yield: 55% (62 mg). X-ray-quality crystals were growth by slow diffusion of diethyl ether into a dichloromethane solution of the complex. Data for **13b** are as follows. IR (CH_2Cl_2): ν 2084 s, 2057 w, 2021 m, 2000 vs cm^{-1} (CO). ^{1}H NMR ($CDCl_3$): δ 7.85−6.90 (m, 20 H, Ph). ^{13}C-{^{1}H} NMR (CH_2Cl_2/D_2O): δ 213.4 (a, *C*O), 212.0 (a, *C*O), 182.1 (s, S_2CNMe_2), 172.3 (a, N*C*CP), 138.6−130.0 (Ph), 76.4 (dd, $^1J_{PC}$ = 49 Hz, $^3J_{PC}$ = 17 Hz, P*C*CN), 50.5 (a, *C*H$_3$), 47.9 (a, *C*H$_3$). ^{31}P{^{1}H} NMR ($CDCl_3$): δ 66.0 (s, a, PPh_2), 25.7 (s, a, PPh_2). Anal. Calcd for $C_{34}H_{26}MnN_3O_5P_2S_2$: C, 55.36; H, 3.55; N, 5.70. Found: C, 55.44; H, 3.67; N, 5.81.

Compound 14. A solution containing $(SCN)_2$ (0.013 g, 0.132 mmol) was added dropwise to a solution of **12** (0.10 g, 0.132 mmol) in 10 mL of CH_2Cl_2 with continuous stirring over 5 min at room temperature. A yellow band was eluted using a hexane/CH_2Cl_2 (1:1.5) mixture. The yellow solid obtained after evaporation of solvents can be recrystallized by diffusion of hexane into a dichloromethane solution of the complex. Data for **14** are as follows. Yield: 20% (0.023 g). IR (CH_2Cl_2): ν 2172 m (CN*t*Bu), 2142 w (SCN), 2029 vs, 1966 s cm^{-1} (CO). ^{1}H NMR ($CDCl_3$): δ 9.14 (d, $^4J_{HH}$ = 2 Hz, H_c), 8.09 (dd, $^3J_{HH}$ = 9 Hz, $^4J_{HH}$ = 2 Hz, H_b), 7.87−7.28 (21 H, H_a + Ph), 1.48 (s, 9 H, *t*Bu). ^{31}P{^{1}H} NMR ($CDCl_3$): δ 69.1 (s, br, PPh_2), 47.2 (s, br, PPh_2). Anal. Calcd for $C_{40}H_{32}MnN_5O_5P_2S_3$: C, 54.86; H, 3.68; N, 8.00. Found: C, 54.74; H, 3.67; N, 8.10.

Compound 15a. A 9 μL portion (0.066 mmol) of HBF_4 (54% diethyl ether complex) was added to 40 mg (0.05 mmol) of **13a** dissolved in 10 mL of dichloromethane. Evaporation of solvents yielded a colorless oil which was washed with diethyl ether (3 × 5 mL), giving a yellow solid which could be recrystallized from a dichloromethane/diethyl ether mixture. Data for **15a** are as follows. Yield: 85% (40 mg). IR (CH_2Cl_2): ν 2178 m (CN*t*Bu), 2052 vs, 1990 s cm^{-1} (CO). IR (Nujol dispersion): 3201 (ν_{N-H}) cm^{-1}. ^{1}H NMR (CD_2Cl_2): δ 7.70−7.21 (41 H, Ph + N-*H*), 1.61 (s, 9 H, *t*Bu). ^{31}P{^{1}H} NMR (CH_2Cl_2/D_2O): δ 101.3 (d, $^2J_{PP}$ = 62 Hz, PPh_2), 34.0 (d, $^2J_{PP}$ = 62 Hz, PPh_2). Anal. Calcd for $C_{38}H_{36}BF_4MnN_4O_4P_2S_2$: C, 51.83; H, 4.12; N, 6.36. Found: C, 51.69; H, 4.20; N, 6.41.

Compound 15b. This compound was prepared similarly to **15a**, using 40 mg (0.054 mmol) of **13b** and 9 μL (0.066 mmol) of HBF_4 (54% diethyl ether complex). Data for **15b** are as follows. Yield: 85% (38 mg). IR (CH_2Cl_2): ν 2100 m, 2041 m, 2017 vs, 1985 s cm^{-1} (CO). ^1H NMR ($CDCl_3$): δ 7.75−7.23 (41 H, Ph + N*H*). $^{31}P\{^1H\}$ NMR ($CDCl_3$): δ 98.5 (br), 30.0 (br). Anal. Calcd for $C_{34}H_{27}BF_4MnN_3O_5P_2S_2$: C, 49.47; H, 3.30; N, 5.09. Found: C, 49.57; H, 3.21; N, 5.20.

Compound 16. This compound was prepared as detailed above, starting with 30 mg (0.034 mmol) of compound **14** and 6 μL (0.044 mmol) of HBF_4. Data for **16** are as follows. Yield: 85% (28 mg). IR (CH_2Cl_2): ν 2173 m (CN*t*Bu), 2052 vs, 1997 s cm^{-1} (CO). IR (Nujol dispersion): 3182 (ν_{N-H}) cm^{-1}. ^1H NMR ($CDCl_3$): δ 9.26 (a, H_c), 8.54 (dd, $^3J_{HH}$ = 8 Hz, $^4J_{HH}$ = 2 Hz, H_b), 8.06 (d, $^3J_{HH}$ = 8 Hz, H_a), 7.67−7.16 (20 H, Ph), 1.61 (s, 9 H, *t*Bu). $^{31}P\{^1H\}$ NMR ($CDCl_3$): δ 101.3 (d, $^2J_{PP}$ = 88 Hz, PPh_2), 51.6 (d, $^2J_{PP}$ = 88 Hz, PPh_2). Anal. Calcd for $C_{40}H_{32}BF_4MnN_5O_5P_2S_3$: C, 49.91; H, 3.45; N, 7.27. Found: C, 50.01; H, 3.52; N, 7.38.

X-ray Crystallography. Crystallographic data for **4**, **5**, **13b,** and **14** are summarized in Table 6. A colorless (**4**, **5)** or yellow (**13b, 14**) prismatic crystal was selected for each experiment. Throughout the experiment Cu Kα radiation was used with a graphite crystal monochromator on a Nonius Kappa-CCD (λ = 1.541 84 Å) single-crystal diffractometer. Unit cell dimensions were determined from the angular settings of a high number of reflections with θ between 3.0 and 70.0° and refined with the programs HKL Denzo and Scalepack.[20] Space groups were determined to be, in all cases, triclinic $P\bar{1}$, from the structure determination. The crystal−detector distance was fixed at 29 mm, and the images were collected using the oscillation method, with a scan oscillation angle of 2.0° and 60 s exposure time per frame. The data collection strategy was calculated with the program Collect.[21] Structure**s** were solved by Patterson methods using DirDif;[22] isotropic least-squares refinements on F^2 were made using SHELXL-97;[23] during the final stages of refinements on F^2 the positional parameters and the anisotropic thermal parameters of the non-H atoms were refined. Figures 1, 2, 4, and 5 were made with ORTEP,[24] showing the atomic numbering schemes. Atomic scattering factors were taken from ref 25. Geometrical calculations were made with PARST.[26]

Acknowledgment. This work was supported by the Spanish Ministerio de Ciencia y Tecnología (PGE and FEDER funding, Project BQU2003-01011). R.Q. thanks the Ministerio de Educación y Ciencia for a contract (Programa Juan de la Cierva).

Supporting Information Available: CIF files giving crystallographic data for **4**, **5**, **13b**, and **14**. This material is available free of charge via the Internet at http://pubs.acs.org.

OM0611195

(20) Otwinowski, Z.; Minor, W. *Methods Enzymol.* **1997**, *276*, 307−326.

(21) Nonius, B. V. Collect; Nonius BV, 1997−2000.

(22) Beurskens, P. T.; Beurskens, G.; de Gelder, R.; García-Granda, S.; Gould, R. O.; Israel, R.; Smits, J. M. M. The DIRDIF-99 Program System; Technical Report of the Crystallography Laboratory, University of Nijmegen, Nijmegen, The Netherlands, 1999.

(23) Sheldrick, G. M. SHELXL97: Program for Crystal Structure Refinement; University of Göttingen, Göttingen, Germany, 1997.

(24) Farrugia, L. J. ORTEP3 for Windows. *J. Appl. Crystallogr.* **1997**, *30*, 565.

(25) *International Tables for Crystallography*; Kynoch Press: Birmingham, U.K., 1992 (present distributor Kluwer Academic Publishers, Dordrecht, The Netherlands); Vol. C, Tables 4.2.6.8 and 6.1.1.4.

(26) Nardelli, M. *J. Appl. Crystallogr.* **1995**, *28*, 659.